Simultaneous nonreciprocal photon blockade via directional parametric amplification

Wei Zhang,[1] Rui Hou,[2] Tie Wang,[2] Shutian Liu,[1,*] Shou Zhang,[2,†] and Hong-Fu Wang[2,‡]
[1]*School of Physics, Harbin Institute of Technology, Harbin, Heilongjiang 150001, China*
[2]*Department of Physics, College of Science, Yanbian University, Yanji, Jilin 133002, China*

(Received 26 March 2024; accepted 12 August 2024; published 22 August 2024)

We propose a scheme to achieve the simultaneous nonreciprocal photon blockade of two microring resonators in an all-optical system without any rotating parts. By unidirectionally parametrically pumping a $\chi^{(2)}$-nonlinear resonator with a classical coherent field, the counterclockwise mode in the resonator is exposed to the parametric amplification process when a forward signal field is input in another resonator, but not the case for a backward signal field. This leads to different quantum interference effects among distinct excitation paths for two optical modes, which is the essential reason for simultaneous nonreciprocal photon blockade. We analytically give the optimal parameter conditions to achieve simultaneous strong photon blockade with the parametric amplification. Furthermore, the nonreciprocity is simultaneously enhanced through tuning the amplitude of input signal. Our work provides an avenue to realize simultaneous nonreciprocal single-photon devices without moving parts and may have potential applications in many-body quantum information processing and quantum communication.

DOI: 10.1103/PhysRevA.110.023723

I. INTRODUCTION

Schemes to create and enhance the photon blockade (PB) effect have been extensively proposed in the past decades, as it played an important role in generating single-photon sources [1–4], which had potential applications in the demonstration of interferometers [5], single-photon transistors [6], and nonclassical isolators [7,8]. Realizing the PB effect was primarily attributed to two physical mechanisms. One was originated from the anharmonic energy-level of the system [1,9–11], causing the prevention of transitions to the two-photon state when the single-photon state was excited, which was known as the conventional photon blockade (CPB). The CPB occurred under the demanding requirement of strong nonlinearity [12,13], which was difficult to implement in practice. To relax the restriction, the quantum destructive interference [14–18] of different excitation pathways from the one-photon state to two-photon state was proposed in diverse systems, called the unconditional photon blockade (UPB). The UPB provided a way to gain insights into quantum correlations even in scenarios with weakly nonlinear coupling [14,18–22].

Essentially, the PB is a process that converts classical light into highly nonclassical light, characterized notably by photon antibunching and sub-Poissonian photon-number statistics [23]. The PB was first experimentally realized in an optical cavity including a single two-level atom [24], marking a pivotal advancement in the realms of quantum optics and laser science. Subsequently, the PB effect has garnered considerable experimental and theoretical interest and made substantial progress in various systems, such as cavity or circuit quantum electrodynamics [10,25,26], cavity optomechanics [11,27–29], magnomechanical systems [30–32], and spinning resonators [33–35]. Specifically, the UPB has been experimentally implemented in coupled optical [21] or superconducting resonators [22]. In addition, many systems have been proven to exhibit the UPB with weak nonlinearities, including two coupled cavities with second- or third-order nonlinearity [36–40] and gain cavity [41].

Nonreciprocal devices, allowing the transmission of signals from one direction while inhibiting them in the opposite direction, have significant applications in building information-processing networks, such as unidirectional transmission [42,43], circulators [44], invisible sensing [45], and noise-free information processing [46]. Thus, a variety of optical nonreciprocal devices have been demonstrated in nonlinear optics [47,48], optomechanics [49,50], magnomechanics [51], and non-Hermitian optics [52,53]. In particular, nonreciprocal entanglement [54,55] and squeezing [56], nonreciprocal phonon and magnon lasers [51,57–61], and nonreciprocal photon blockade (NPB) have been proposed based on various schemes. Among them, nonreciprocal CPB (NCPB) [33] and nonreciprocal UPB (NUPB) [34] were first achieved in a spinning resonator, respectively based on the mechanisms of energy-level anharmonicity and quantum destructive interference. Subsequently, NCPB [62,63] and NUPB [63,64] occur in a spinning resonator coupled to a two-level atom. In addition, NPBs were observed in a two-mode cavity made of $\chi^{(2)}$ nonlinear materials [65], a rotating optomechanical system [34,66], and a driven dissipative cavity featuring parametric amplification [67]. Very recently, simultaneous NPB [68,69] of two resonators were proposed attributing to the Fizeau drags of two spinning resonators. However, utilizing the directional parametric amplification to simultaneously generate NPB of two resonators has not

*Contact author: stliu@hit.edu.cn
†Contact author: szhang@ybu.edu.cn
‡Contact author: hfwang@ybu.edu.cn

yet been explored, which greatly simplifies its experimental implementation.

In this paper, we consider an all-optical system consisting of two coupled microring resonators and two nearby optical waveguides to investigate simultaneous generation of NPB in two optical modes. Our scheme exhibits notable differences and advantages across various aspects in contrast to Ref. [69]. (i) The results of simultaneous NPB are completely different, as the all-optical system with directional parametric amplification gives rise to different transition pathways, thereby causing different physical mechanisms. (ii) The adjustment of the nonreciprocity is easier, as it only requires adjusting the gain and phase of parametric amplification, without involving the radius and linear refractive index of resonator, and angular velocities of spinning resonators. (iii) A better nonreciprocal ratio (95 dB) for photon blockade of two modes can be realized in our scheme with a smaller signal-field amplitude under the condition of the optimal parametric amplification and phase. (iv) The method of using directional parametric amplification to generate simultaneous NPB requires fewer experimental equipment and steps, which is easier to implement in experiments. Specifically, by coherently pumping a resonator to induce a parametric amplification process in one direction but not the other, different interference pathways are induced for two distinct end inputs, leading to the occurrence or disappearance of quantum destructive interference in excitation pathways to access the two-photon states. We analytically derive the optimal conditions for achieving strong photon antibunching in two resonators with the parametric amplification and demonstrate that the analytical solutions show a great agreement with the numerical simulations. Based on these conditions, it is found that the simultaneous NPB is significantly influenced by the coupling strength and input signal-field strength. Our work offers a way for simultaneously achieving strong nonreciprocal single-photon devices in multiple modes without the need for any rotating components, which holds promise for applications in many-body quantum information processing and quantum communication.

The paper is organized as follows. Section II details the basic framework of an all-optical system under study, which mainly consists of the corresponding Hamiltonian and master equation. Section III derives the optimal parameter conditions for simultaneous photon blockade in the presence of the parametric amplification. Section IV investigates the simultaneous NPB of two resonators and discusses how to improve the nonreciprocity. Finally, we give a conclusion in Sec. V.

II. SYSTEM MODEL AND THEORETICAL FRAMEWORK

As schematically shown in Fig. 1, we consider two coupled microring resonators made of high-quality $\chi^{(2)}$ nonlinear thin film and two nearby optical waveguides. Due to the nonlinear parametric amplification process supported by the resonators, the counterclockwise (CCW) mode in resonator B (R_B) $b_{\circlearrowleft}$ is exposed to the parametric interaction under the directional phase-matching condition when R_B is pumped from port 3 by a coherent laser field with amplitude Ω_p, frequency ω_p, and phase θ_p. However, the clockwise (CW) mode $b_{\circlearrowright}$ in R_B is decoupled due to the lack of the phase-matching condition. In Fig. 1(a), a driving field with amplitude E and frequency ω_l

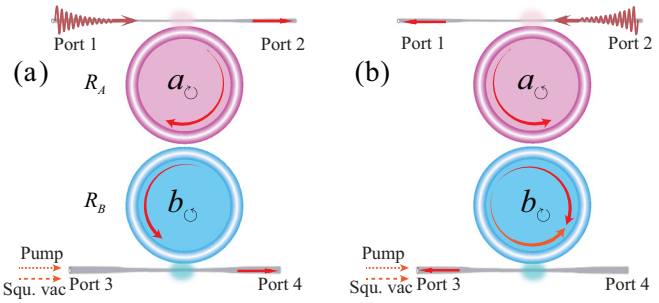

FIG. 1. Schematic of a coupled-resonators system generating simultaneous NPB, which consists of two microring resonators (R_A and R_B) and two nearby optical waveguides. To achieve the simultaneous NPB of two optical modes, a coherent pump field is applied to generate a CCW mode $b_{\circlearrowleft}$ in R_B. To eliminate the increased dissipation brought by the pump field, a broadband squeezed-vacuum field is used to drive R_B. (a) A forward-input signal field excites the CW mode $a_{\circlearrowright}$ in R_A coupled to the CCW mode $b_{\circlearrowleft}$ in R_B. (b) A backward-input signal field excites the CCW mode $a_{\circlearrowleft}$ in R_A, which interacts with the CW mode $b_{\circlearrowright}$ in R_B.

loaded from port 1 excites the CW mode $a_{\circlearrowright}$ in resonator A (R_A), which couples to $b_{\circlearrowright}$ with the hopping strength of g. In this case, the system Hamiltonian with the respect to the frame rotating at frequency $\omega_p/2$ is expressed as ($\hbar = 1$)

$$H_1 = \Delta_a a_{\circlearrowright}^\dagger a_{\circlearrowright} + \Delta_b b_{\circlearrowright}^\dagger b_{\circlearrowright} + g(a_{\circlearrowright}^\dagger b_{\circlearrowright} + a_{\circlearrowright} b_{\circlearrowright}^\dagger) + E(a_{\circlearrowright}^\dagger + a_{\circlearrowright}) + \Omega_p(e^{-i\theta_p} b_{\circlearrowright}^{\dagger 2} + e^{i\theta_p} b_{\circlearrowright}^2), \quad (1)$$

where $a_{\circlearrowright}$ ($a_{\circlearrowright}^\dagger$) and $b_{\circlearrowright}$ ($b_{\circlearrowright}^\dagger$) represent the annihilation (creation) operators of the CW mode in R_A and the CCW mode in R_B, respectively. $\Delta_{a,b} = \omega_{a,b} - \omega_p/2$, with $\omega_{a,b}$ being the frequencies of R_A and R_B. Here we assume $\omega_p = 2\omega_l$. When the driving field is input from port 2 as shown in Fig. 1(b), the CCW mode $a_{\circlearrowleft}$ in R_A is excited and couples to CW mode $b_{\circlearrowright}$ in R_B. In this situation, the system Hamiltonian is written as

$$H_2 = \Delta_a a_{\circlearrowleft}^\dagger a_{\circlearrowleft} + \Delta_b b_{\circlearrowright}^\dagger b_{\circlearrowright} + g(a_{\circlearrowleft}^\dagger b_{\circlearrowright} + a_{\circlearrowleft} b_{\circlearrowright}^\dagger) + E(a_{\circlearrowleft}^\dagger + a_{\circlearrowleft}). \quad (2)$$

Next we will demonstrate that, owing to the directional parametric amplification, the simultaneous NPB of two resonators can be achieved when the driving field is loaded from port 1 or port 2. Via considering the dissipation terms of two resonators, the dynamics of the hybrid system can be characterized by the following master equation:

$$\dot{\rho} = -i[H_\zeta, \rho] + \kappa_a \mathcal{L}[a_\zeta]\rho + \kappa_b \mathcal{L}[b_\zeta]\rho, \quad (3)$$

where ρ is the system density operator, $\mathcal{L}[o]\rho = o\rho o^\dagger - (o^\dagger o\rho + \rho o^\dagger o)/2$ ($o = a_\zeta, b_\zeta$) is the Lindblad superoperator for operator o. κ_a (κ_b) is the total decay rate of R_A (R_B). For the sake of simplicity, it is taken to be $\kappa_a = \kappa_b$ hereafter. $\zeta = 1, 2$ indicates the driving-field inputs from ports 1 and 2, respectively. a_1 (b_1) denotes $a_{\circlearrowright}$ ($b_{\circlearrowright}$), and a_2 (b_2) represents $a_{\circlearrowleft}$ ($b_{\circlearrowleft}$). For the two situations where the driving field is input from ports 1 and 2, the photon blockade effect of two resonators can be quantified by the equal-time second-order

correlation function

$$g^{(2)}_{a_\zeta}(0)=\frac{\langle a^{\dagger 2}_\zeta a^2_\zeta\rangle}{\langle a^\dagger_\zeta a_\zeta\rangle^2}=\frac{\mathrm{Tr}\left(\rho_{ss}a^{\dagger 2}_\zeta a^2_\zeta\right)}{[\mathrm{Tr}(\rho_{ss}a^\dagger_\zeta a_\zeta)]^2},$$
$$g^{(2)}_{b_\zeta}(0)=\frac{\langle b^{\dagger 2}_\zeta b^2_\zeta\rangle}{\langle b^\dagger_\zeta b_\zeta\rangle^2}=\frac{\mathrm{Tr}\left(\rho_{ss}b^{\dagger 2}_\zeta b^2_\zeta\right)}{[\mathrm{Tr}(\rho_{ss}b^\dagger_\zeta b_\zeta)]^2}, \tag{4}$$

where ρ_{ss} is the steady-state density operator of master equation (5) by taking $\dot{\rho}=0$. Generally, the value of $g^{(2)}_o(0)$ signifies the probability of observing two photons at the same time. Typically, $g^{(2)}_o(0)<1$ implies that the photon is detected one by one, corresponding to the photon antibunching effect. However, $g^{(2)}_o(0)>1$ describes the photon bunching effect, meaning that two photons can be simultaneously detected.

III. OPTIMAL CONDITIONS FOR PHOTON BLOCKADE WITH PARAMETRIC AMPLIFICATION

In this part, we are mainly interested in the optimal conditions for photon blockade of the two resonators with the parametric amplification when the R_A is weakly driven. Before giving a full discussion of the simultaneous NPB, we first derive the analytical solutions by solving the Schrödinger equation $i\partial|\psi\rangle/\partial t=H_{\mathrm{non}}|\psi\rangle$, where

$$H_{\mathrm{non}}=H_1-i\frac{\kappa_a}{2}a^\dagger_1a_1-i\frac{\kappa_b}{2}b^\dagger_1b_1, \tag{5}$$

and $|\psi\rangle$ is the wave function of the system, which can be truncated to two excitation subspaces in the weak driving field limit (E, $\Omega_p\ll\kappa_a,\kappa_b$). In the truncated space, the steady-state wave function can be written as the form

$$|\psi\rangle=C_{00}|00\rangle+C_{10}|10\rangle+C_{01}|01\rangle+C_{20}|20\rangle+C_{11}|11\rangle+C_{02}|02\rangle, \tag{6}$$

where $|C_{ab}|^2$ represents the probability of the occupation staying in state $|ab\rangle$. $|ab\rangle=|a\rangle\otimes|b\rangle$ is a direct product state, which means that there are a photons of CW mode in R_A and b photons of CCW mode in R_B. It is worth mentioning that Eq. (6) is a hypothesis describing the evolution of the system. We will further demonstrate the validity of the hypothesis by the numerical simulations in the next section. Substituting the non-Hermitian Hamiltonian (5) and wave function (6) into the Schrödinger equation, a set of dynamical equations of the occupying probabilities can be obtained as

$$\begin{aligned}
i\dot{C}_{00}&=EC_{10}+\sqrt{2}\Omega_pe^{i\theta_p}C_{02},\\
i\dot{C}_{10}&=\tilde{\Delta}_aC_{10}+gC_{01}+EC_{00}+\sqrt{2}EC_{20},\\
i\dot{C}_{01}&=\tilde{\Delta}_bC_{01}+gC_{10}+EC_{11},\\
i\dot{C}_{20}&=2\tilde{\Delta}_aC_{20}+\sqrt{2}gC_{11}+\sqrt{2}EC_{10},\\
i\dot{C}_{11}&=(\tilde{\Delta}_a+\tilde{\Delta}_b)C_{11}+\sqrt{2}g(C_{20}+C_{02})+EC_{01},\\
i\dot{C}_{02}&=2\tilde{\Delta}_bC_{02}+\sqrt{2}gC_{11}+\sqrt{2}\Omega_pe^{-i\theta_p}C_{00},
\end{aligned} \tag{7}$$

where $\tilde{\Delta}_{a(b)}=\Delta_{a(b)}-i\kappa_{a(b)}$. By setting $\dot{C}_{ab}=0$, all probability amplitudes in the steady state can be solved. To obtain a perfect photon blockade in two resonators, the two-photon probability amplitudes in two modes are equal to zero. Thus

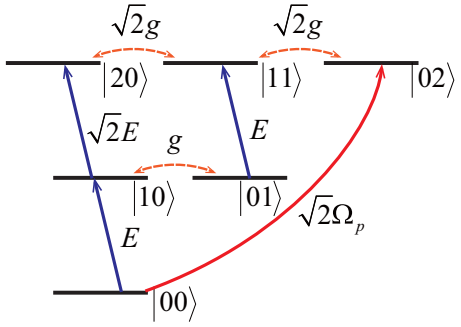

FIG. 2. Energy-level diagram of the system in the forward input case, showing the zero-, one-, and two-photon states (horizontal black lines without arrows) and the corresponding transition pathways (color lines with arrows) leading to the destructive interference for preventing the two-photon occupation.

we consider $C_{20}=0$ and $C_{02}=0$, and further arrive at

$$\begin{aligned}
\tilde{\Delta}_aC_{10}+gC_{01}+EC_{00}&=0,\\
\tilde{\Delta}_bC_{01}+gC_{10}+EC_{11}&=0,\\
\sqrt{2}gC_{11}+\sqrt{2}EC_{10}&=0,\\
(\tilde{\Delta}_a+\tilde{\Delta}_b)C_{11}+EC_{01}&=0,\\
\sqrt{2}gC_{11}+\sqrt{2}\Omega_pe^{-i\theta_p}C_{00}&=0.
\end{aligned} \tag{8}$$

It is worth noting that, in the absence of the parametric amplification, i.e., $\Omega_p=0$, no nontrivial solution can be obtained from Eq. (8). This may imply that the parametric amplification plays an essential role in generating the simultaneous NPB. Utilizing these equations, we can derive the optimal conditions, which are necessary but insufficient. Specifically, we use C_{11} to represent C_{10}, C_{01}, and C_{00} of the third, fourth, and fifth equations above, and then introduce C_{10}, C_{01}, and C_{00} into the first equation of Eq. (8). Thus, we can obtain $\Omega_pe^{-i\theta_p}=-\frac{E^2}{2\tilde{\Delta}_a+\tilde{\Delta}_b}$, which is equivalent to the following two equations:

$$\Omega_p^{\mathrm{opt}}=\mathrm{Abs}\left[-\frac{E^2}{2\tilde{\Delta}_a+\tilde{\Delta}_b}\right],\quad \theta_p^{\mathrm{opt}}=-\mathrm{Arg}\left[-\frac{E^2}{2\tilde{\Delta}_a+\tilde{\Delta}_b}\right]. \tag{9}$$

Therefore, we derive the optimal equations required for photon blockade in the two modes. The conditions in Eq. (9) ensure that $C_{20}=0$ and $C_{02}=0$ are simultaneously satisfied. This indicates that the two-photon states $|20\rangle$ and $|02\rangle$ can be simultaneously eliminated due to the quantum destructive interference between different transition pathways. Specifically, as shown in Fig. 2, there are three excitation paths to access the two-photon state $|20\rangle$: one direct excitation in Fig. 2(a) $|10\rangle\xrightarrow{\sqrt{2}E}|20\rangle$, and two indirect excitations in Figs. 2(b) $|10\rangle\xrightarrow{g}|01\rangle\xrightarrow{E}|11\rangle\xrightarrow{\sqrt{2}g}|20\rangle$ and 2(c) $|00\rangle\xrightarrow{\sqrt{2}\Omega_p}|02\rangle\xrightarrow{\sqrt{2}g}|11\rangle\xrightarrow{\sqrt{2}g}|20\rangle$. Likewise, there are one direct excitation and two indirect excitations to reach the two-photon state $|02\rangle$: [Fig. 2(a)] $|00\rangle\xrightarrow{\sqrt{2}\Omega_p}|02\rangle$, [Fig. 2(b)] $|10\rangle\xrightarrow{g}|01\rangle\xrightarrow{E}|11\rangle\xrightarrow{\sqrt{2}g}|02\rangle$, and [Fig. 2(c)] $|10\rangle\xrightarrow{\sqrt{2}E}|20\rangle\xrightarrow{\sqrt{2}g}$

$|11\rangle \xrightarrow{\sqrt{2}g} |02\rangle$. As analytically calculated above, $C_{20} = 0$ and $C_{02} = 0$ guarantee strong simultaneous photon blockade in two modes under the optimal parametric amplification $\Omega_p^{\rm opt}$ and phase $\theta_p^{\rm opt}$ since the two-photon states can be completely inhibited through the destructive interference.

Next we derive the optimal expressions for driving detunings Δ_a and Δ_b based on the optimal conditions in Eq. (9) and further give the analytical expressions for second-order correlation functions. With the condition $C_{00} \simeq 1 \gg C_{10}, C_{01} \gg C_{11}, C_{20}, C_{02}$, and neglecting the terms of C_{20} and C_{11} of the second and third equations in Eq. (7), single excitation and two excitation coefficients in the steady state can be solved as

$$
\begin{aligned}
C_{10} &= \frac{\tilde{\Delta}_b E}{g^2 - \tilde{\Delta}_a\tilde{\Delta}_b},\\
C_{01} &= \frac{-gE}{g^2 - \tilde{\Delta}_a\tilde{\Delta}_b},\\
C_{20} &= \frac{\tilde{\Delta}_b^2(\tilde{\Delta}_a + \tilde{\Delta}_b)E^2 + g^2(g^2 - \tilde{\Delta}_a\tilde{\Delta}_b)\Omega_p e^{-i\theta_p}}{Z},\\
C_{11} &= \frac{\sqrt{2}g}{Z}[\tilde{\Delta}_a(\tilde{\Delta}_a\tilde{\Delta}_b - g^2)\Omega_p e^{-i\theta_p} - \tilde{\Delta}_b(\tilde{\Delta}_a + \tilde{\Delta}_b)E^2],\\
C_{02} &= \frac{1}{Z}\{(\tilde{\Delta}_a + \tilde{\Delta}_b)g^2E^2 - (g^2 - \tilde{\Delta}_a\tilde{\Delta}_b)\\
&\quad \times [g^2 - \tilde{\Delta}_a(\tilde{\Delta}_a + \tilde{\Delta}_b)]\Omega_p e^{-i\theta_p}\},
\end{aligned}
\tag{10}
$$

where $Z = \sqrt{2}(\tilde{\Delta}_a + \tilde{\Delta}_b)(g^2 - \tilde{\Delta}_a\tilde{\Delta}_b)^2$. Hence the statistical characteristic of two-photon modes can be analytically expressed via the steady-state probability amplitudes as

$$
\begin{aligned}
g^{(2)}_{a_\zeta}(0) &= \frac{2|C_{20}|^2}{(|C_{10}|^2 + 2|C_{20}|^2 + |C_{11}|^2)^2} \approx \frac{2|C_{20}|^2}{|C_{10}|^4},\\
g^{(2)}_{b_\zeta}(0) &= \frac{2|C_{02}|^2}{(|C_{01}|^2 + 2|C_{02}|^2 + |C_{11}|^2)^2} \approx \frac{2|C_{02}|^2}{|C_{01}|^4}.
\end{aligned}
\tag{11}
$$

Then, the realization of $g^{(2)}_{a_\zeta}(0) \longrightarrow 0$ and and $g^{(2)}_{b_\zeta}(0) \longrightarrow 0$ requires $C_{20} = 0$ and $C_{02} = 0$, respectively. Introducing the optimal $\Omega_p^{\rm opt}$ and $\theta_p^{\rm opt}$ of Eq. (9), one can obtain the optimal detuning expression for the strong blockade in mode a_1 under the condition of $\Delta_a, \Delta_b \gg \kappa_a, \kappa_b$,

$$
(\Delta_a + \Delta_b)(2\Delta_a + \Delta_b)\Delta_b^2 - g^2(g^2 - \Delta_a\Delta_b) = 0. \tag{12}
$$

In a similar manner, we set $C_{02} = 0$ and introduce $\Omega_p^{\rm opt}$ and $\theta_p^{\rm opt}$. Then we obtain the optimal condition for strong blockade in mode b_1

$$
\begin{aligned}
&(\Delta_a + \Delta_b)(2\Delta_a + \Delta_b)g^2 - (g^2 - \Delta_a\Delta_b)\\
&\quad \times [g^2 - \Delta_a(\Delta_a + \Delta_b)] = 0.
\end{aligned}
\tag{13}
$$

It is worth pointing out that the optimal detunings are required for $C_{20} = 0$ and $C_{02} = 0$. For a fixed g, $\Delta_a^{\rm opt}$ and $\Delta_b^{\rm opt}$ in strong photon antibunching for a_1 and b_1 can be obtained from Eqs. (12) and (13). However, the solutions are too cumbersome to be shown here. In other words, the strong photon antibunching can be simultaneously achieved in two resonators under the optimal parameter condition $(\Omega_p^{\rm opt}, \theta_p^{\rm opt}, \Delta_a^{\rm opt}, \Delta_b^{\rm opt})$. In the following section, we discuss the effect of different parameters on simultaneous NPB when the driving field is from distinct port inputs.

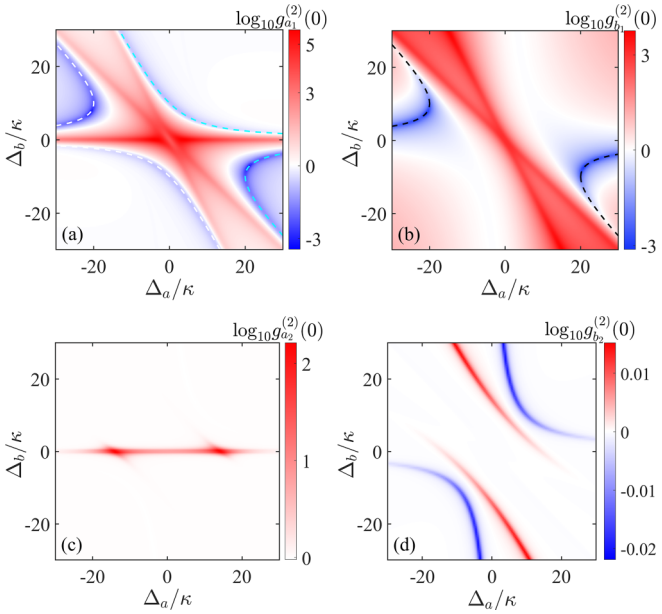

FIG. 3. Second-order correlation function on a logarithmic scale $\log_{10}[g_o^{(2)}(0)]$ as a function of Δ_a/κ and Δ_b/κ for the forward input cases (a) and (b), and the backward input cases (c) and (d). In the unit of κ, we take $g = 10\kappa$ and $E = 0.1\kappa$. Ω_p and θ_p are taken according to Eq. (9).

IV. SIMULTANEOUS NPB IN TWO RESONATORS

In this section, we demonstrate how the simultaneous NPB in two modes are realized when the input of the driving field converts from port 1 to port 2, implying that the parametric amplification changes from presence to absence. The photon statistics are characterized by the correlations as given in Eq. (4), which can be achieved by numerically solving the master equation (3) utilizing the PYTHON package QUTIP [70].

To check the validity of the above analytical derivation, we plot the steady-state logarithmic equal-time second-order correlation function $\log_{10}g^{(2)}_{a_1}(0)$ and $\log_{10}g^{(2)}_{b_1}(0)$ as a function of Δ_a/κ and Δ_b/κ in Figs. 3(a) and 3(b) for the case of input from port 1, respectively. In the unit of κ, we take $g = 10\kappa$ and $E = 0.1\kappa$. It can be observed that under the optimal detuning condition given by Eqs. (12) and (13), the simultaneous strong photon blockade for two resonators appears in the blue areas. The white and cyan dashed curves correspond to the two solutions according to Eq. (12), and the black dashed curves represent the two solutions according to Eq. (13). We find that a part of the white and cyan curves occur in the same areas as the black curves, implying the simultaneous strong PB. When the driving field is input from port 2 in which the two-photon driving applied to the R_B is absent, $\log_{10}g^{(2)}_{a_2}(0)$ and $\log_{10}g^{(2)}_{b_2}(0)$ as a function of Δ_a/κ and Δ_b/κ are respectively plotted in Figs. 3(c) and 3(d). It can be seen that $\log_{10}g^{(2)}_{a_2}(0) > 0$ and $\log_{10}g^{(2)}_{b_2}(0) > 0$ in almost the entire parameter regions. That is to say, when the driving field is input from different

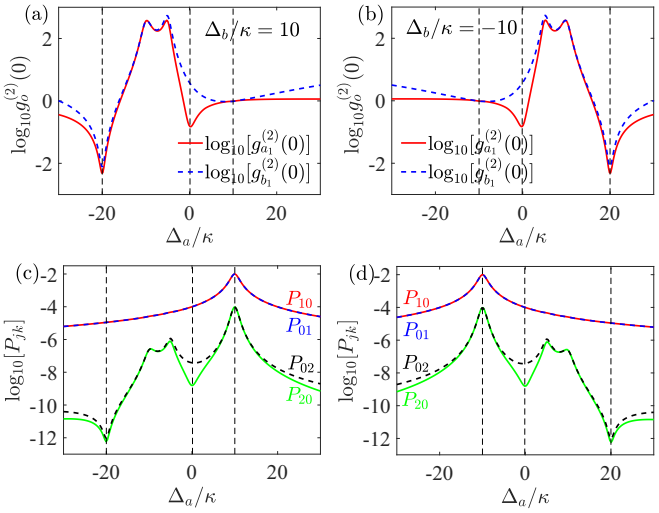

FIG. 4. Second-order correlation function on a logarithmic scale $\log_{10}[g_{a_1}^{(2)}(0)]$ and $\log_{10}[g_{b_1}^{(2)}(0)]$ as a function of Δ_a/κ in (a) with $\Delta_b/\kappa = 10$ and in (b) with $\Delta_b/\kappa = -10$. $\log_{10}[P_{jk}]$ is plotted in (c) with $\Delta_b/\kappa = 10$ and in (d) with $\Delta_b/\kappa = -10$. The other parameters are the same as given in Fig. 3.

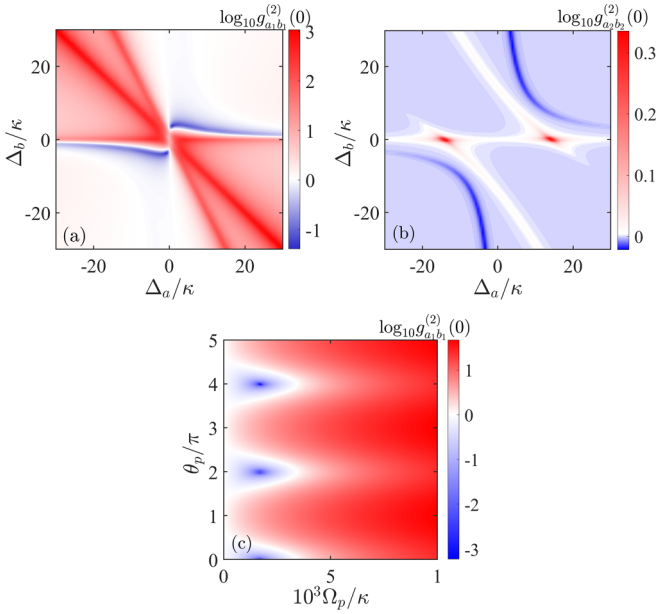

FIG. 5. Cross-correlation functions $\log_{10}g_{a_1b_1}^{(2)}(0)$ (a) and $\log_{10}g_{a_2b_2}^{(2)}(0)$ (b) as a function of Δ_a/κ and Δ_b/κ under the condition of Eq. (9). (c) $\log_{10}g_{a_1b_1}^{(2)}(0)$ as a function of Ω_p/κ and θ_p/π when $\Delta_a/\kappa = 10$ and $\Delta_b = -\Delta_a/3$ are taken. The other parameters are the same as given in Fig. 3.

ports 1 or 2, the directional parametric amplification holds a significant responsibility for the simultaneous NPB.

To make a clearer illustration, we depict the second-order correlation functions $\log_{10}g_{a_1}^{(2)}(0)$ and $\log_{10}g_{b_1}^{(2)}(0)$ as a function of Δ_a/κ for $\Delta_b = 10\kappa$ in Fig. 4(a) and for $\Delta_b = -10\kappa$ in Fig. 4(b). For input from distinct ports, resulting in the presence or absence of the parametric amplification, the correlation functions for modes a and b are simultaneously nonreciprocal [$\log_{10}g_{a_2}^{(2)}(0) = 0$ and $\log_{10}g_{b_2}^{(2)}(0) = 0$, which are not shown here]. It is inferred that the lack of Ω_p leads to the absence of perfect destructive interference among the transition paths. When the optimal parameter conditions $\Omega_p^{\rm opt}$ and $\theta_p^{\rm opt}$ are taken according to Eq. (9), we observe that the two optical modes show a simultaneous strong antibunching effect at optimal detuning $\Delta_a/\kappa = -20$ in Fig. 4(a). In addition, we find that there is another optimal detuning $\Delta_a/\kappa \approx 0$ for a strong antibunching effect in the CW mode a_1. In Fig. 4(b), the optimal detunings locate at $\Delta_a/\kappa = 0, 20$ due to the variation of Δ_b/κ, which is required by the optimal condition based on Eqs. (12) and (13). Furthermore, the state occupations $P_{jk} = |\langle jk|\psi\rangle|^2$ $(j, k = 0, 1, 2)$ are plotted in Fig. 4(c) for $\Delta_b/\kappa = 10$ and in Fig. 4(d) for $\Delta_b/\kappa = -10$. It is seen that $\Delta_a/\kappa = -20$ in Fig. 4(c) and $\Delta_a/\kappa = 20$ in Fig. 4(d) are the dips of states $|20\rangle$ and $|02\rangle$, which accounts for $\Delta_a/\kappa = -20$ in Fig. 4(a) and $\Delta_a/\kappa = 20$ in Fig. 4(b) are the optimal detunings for the photon antibunching. In addition, the curve trends of P_{20} and P_{02} are the same as those of $\log_{10}g_{a_1}^{(2)}(0)$ and $\log_{10}g_{b_1}^{(2)}(0)$, respectively. This demonstrates that the generated strong photon antibunching effect originates from quantum destructive interference between different transition paths to reach the states $|20\rangle$ and $|02\rangle$.

To further investigate the anticorrelation effect between photons and photons, in Fig. 5, we plot the second-order cross-correlation function $g_{a_\zeta b_\zeta}^{(2)}(0)$, which is defined as

$$g_{a_\zeta b_\zeta}^{(2)}(0) = \frac{\langle a_\zeta^\dagger b_\zeta^\dagger b_\zeta a_\zeta\rangle}{\langle a_\zeta^\dagger a_\zeta\rangle\langle b_\zeta^\dagger b_\zeta\rangle} = \frac{{\rm Tr}(\rho_{ss}a_\zeta^\dagger b_\zeta^\dagger b_\zeta a_\zeta)}{[{\rm Tr}(\rho_{ss}a_\zeta^\dagger a_\zeta)][{\rm Tr}(\rho_{ss}b_\zeta^\dagger b_\zeta)]}. \tag{14}$$

$g_{a_\zeta b_\zeta}^{(2)}(0) < 1$ indicates that one photon in mode a and one photon in mode b cannot exist simultaneously, which is called the anticorrelation of the photon and photon. On the contrary, $g_{a_\zeta b_\zeta}^{(2)}(0) > 1$ implies that the photon in mode a and photon in mode b tend to bunch together. In Figs. 5(a) and 5(b), $\log_{10}g_{a_1b_1}^{(2)}(0)$ and $\log_{10}g_{a_2b_2}^{(2)}(0)$ are plotted under the condition of Eq. (9), respectively. It can be found that the cross-correlation functions exhibit a strong nonreciprocal feature, where $\log_{10}g_{a_1b_1}^{(2)}(0) < 0$ and $\log_{10}g_{a_2b_2}^{(2)}(0) > 0$ occur in the same parameter area. Furthermore, we find that the parameter region of $\log_{10}g_{a_1b_1}^{(2)}(0) < 0$ is the region of $\log_{10}g_{a_1}^{(2)}(0) > 0$ and $\log_{10}g_{b_1}^{(2)}(0) > 0$, which demonstrates that the cross correlation between the modes exhibits strong antibunching while there is bunching in modes a_1 and b_1. In contrast, the parameter region of $\log_{10}g_{a_1b_1}^{(2)}(0) > 0$ is the region of $\log_{10}g_{a_1}^{(2)}(0) < 0$ and $\log_{10}g_{b_1}^{(2)}(0) < 0$, which shows that the cross correlation between the modes exhibits bunching while there is strong antibunching in modes a_1 and b_1. In Fig. 5(c), we investigate the influence of Ω_p and θ_p on $\log_{10}g_{a_1b_1}^{(2)}(0)$. The results show that the absence of the parametric amplification implies no anticorrelation effect under the current parameter condition. Additionally, a stronger antibunching effect appears around $\Omega_p/\kappa = 2 \times 10^{-3}$ and $\theta_p = n\pi$ (n being even), corresponding to the cross-correlation function value of $\log_{10}g_{a_1b_1}^{(2)}(0) \approx 10^{-3}$.

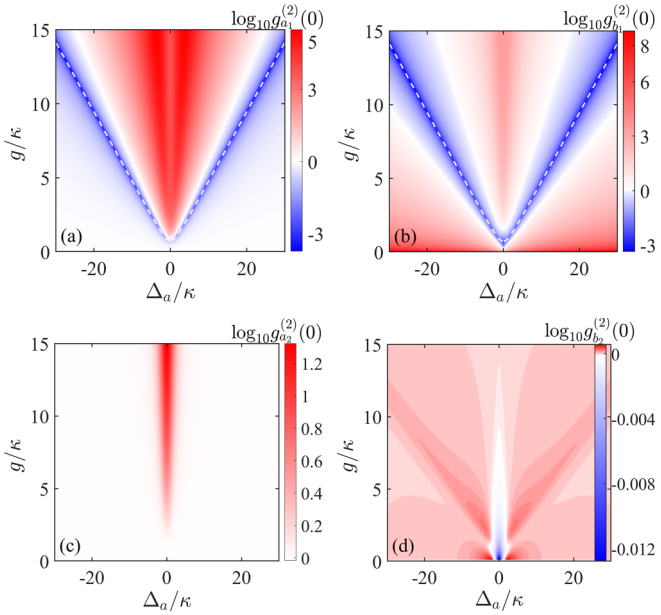

FIG. 6. Second-order correlation function on a logarithmic scale $\log_{10}[g_o^{(2)}(0)]$ as a function of Δ_a/κ and g/κ for the forward input cases (a) and (b), and the backward input cases (c) and (d). In all the plots, $\Delta_b = -\Delta_a/3$ is used. The other parameters are the same as given in Fig. 3.

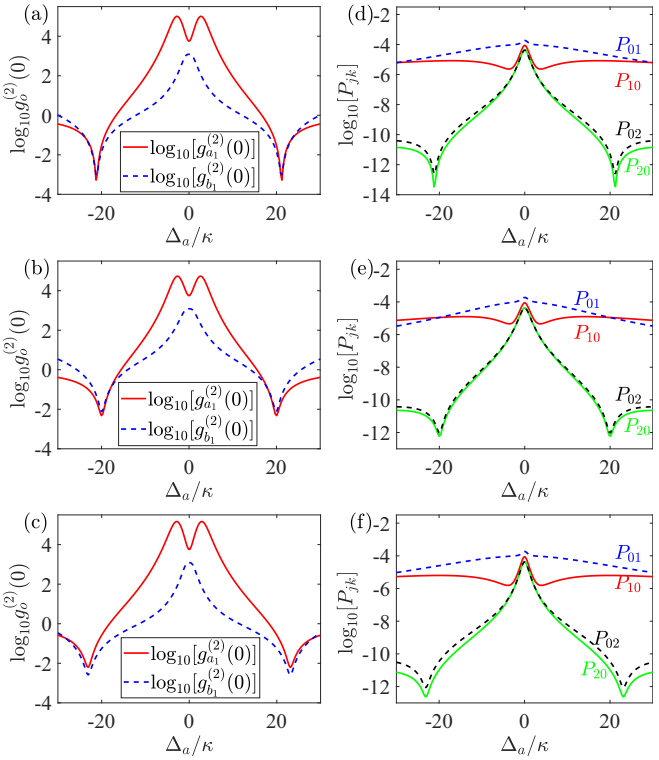

FIG. 7. (a)–(c) Second-order correlation function on a logarithmic scale $\log_{10}[g_{a_1}^{(2)}(0)]$ and $\log_{10}[g_{b_1}^{(2)}(0)]$, and (d)–(f) $\log_{10}[P_{jk}]$ as a function of Δ_a/κ. $\Delta_b/\kappa = -\Delta_a/3$, $\Delta_b = -\Delta_a/2$, and $\Delta_b = -\Delta_a/4$ are taken in (a) and (d), (b) and (e), (c) and (f), respectively. The other parameters are the same as given in Fig. 3.

Next, we give the optimal parameter condition for simultaneous strong photon blockade from another perspective. Based on the third equation in Eq. (10), we directly set $C_{20} = 0$ and introduce the optimal Ω_p and θ_p. Thus we obtain

$$(2\tilde{\Delta}_a + \tilde{\Delta}_b)(\tilde{\Delta}_a + \tilde{\Delta}_b)\tilde{\Delta}_b^2 - g^2(g^2 - \tilde{\Delta}_a\tilde{\Delta}_b) = 0. \quad (15)$$

By decomposing both the real and imaginary parts equal to zero, we can obtain the solutions of the above equation

$$\Delta_a = \pm\tfrac{3}{2}\sqrt{2g^2 - \kappa^2}, \quad \Delta_b = -\tfrac{1}{3}\Delta_a. \quad (16)$$

The conditions in Eq. (16) are also valid for $C_{02} = 0$. In the following discussion, we validate the consistency of analytical solution and numerical simulation. Figures 6(a) and 6(b) show the equal-time second-order correlation function $\log_{10}[g_{a_1}^{(2)}(0)]$ and $\log_{10}[g_{b_1}^{(2)}(0)]$ as a function of the detuning Δ_a/κ and coupling g/κ, respectively. The white dashed lines denote $\Delta_a = \pm 3/2\sqrt{2g^2 - \kappa^2}$ occurring in the areas of strong photon antibunching, which proves that the analytical optimal condition in Eq. (16) is in great agreement with the numerical results. As expected, when Ω_p is absent due to the input from port 2, there is no photon blockade phenomenon in two modes, as shown in Figs. 6(c) and 6(d), which shows a good nonreciprocity for the two modes.

To clearly demonstrate the superiority of Eq. (16), $\log_{10}[g_o^{(2)}(0)]$ and $\log_{10}[P_{jk}]$ are plotted as a function of Δ_a/κ in Figs. 7(a) to 7(c) and Figs. 7(d) to 7(f), respectively. Here $\Delta_b = -\Delta_a/3$ is taken in Figs. 7(a) and 7(d), $\Delta_b = -\Delta_a/2$ is taken Figs. 7(b) and 7(e), and $\Delta_b = -\Delta_a/4$ is taken in Figs. 7(c) and 7(f). Compared with the results in Figs. 7(b) and 7(c), $\log_{10}[g_o^{(2)}(0)]$ is largely decreased by approximately one order of magnitude with $\Delta_b = -\Delta_a/3$. In addition, the optimal detunings are determined by the first equation in Eq. (16). Moreover, we find that with $\Delta_b = -\Delta_a/4$, there exists $\log_{10}[g_{b_1}^{(2)}(0)] < \log_{10}[g_{a_1}^{(2)}(0)]$, which means that a stronger antibunching effect for mode b can be achieved by tuning the parameters.

To quantitatively measure the NPB of two modes, we define the nonreciprocal ratio for mode o as

$$I_o = -10\log_{10}\left[\frac{g_{o,\Omega_p\neq 0}^{(2)}(0)}{g_{o,\Omega_p=0}^{(2)}(0)}\right]. \quad (17)$$

It provides the ratio of photon correlation functions from two distinct input ends, which means that the ratio of photon correlation functions under the presence and absence of the parametric amplification Ω_p. The utilization of the ratio stems from the characteristics of photon statistics under the optimal parameters discussed above, i.e., $g_o^{(2)}(0) \ll 1$ with $\Omega_p^{\rm opt}$ and $g_o^{(2)}(0) \sim 1$ without Ω_p. From Fig. 8(a), we see that a larger coupling strength g generates a better nonreciprocity for both modes, where we use $I_{o,\rm opt}$ to represent the nonreciprocal ratio under the optimal parameters. This is because that a large g involved in key excitation paths can enhance the quantum destructive interference, leading to a smaller $g_{a_1}^{(2)}(0)$ and $g_{b_1}^{(2)}(0)$. However, this is not sufficient to demonstrate the nonreciprocity, to do this, we display the

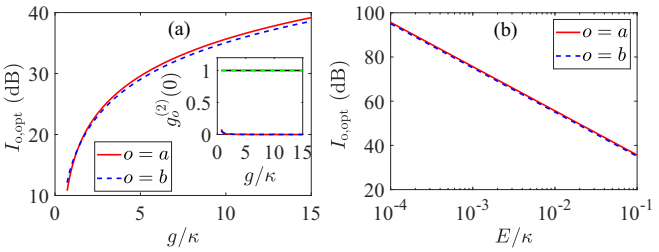

FIG. 8. The nonreciprocal ratio $I_{o,\mathrm{opt}}$ $(o=a,b)$ as a function of (a) coupling strength g/κ and (b) driving field amplitude E/κ. The inset in (a) plots the second-order correlation functions $g_o^{(2)}(0)$ as a function of g/κ. Δ_a and Δ_b are taken according to Eq. (16). The other parameters are the same as given in Fig. 3.

dependence of photon correlation functions $g_o^{(2)}(0)$ on g under the same conditions. When Ω_p^{opt} and θ_p^{opt} are utilized, $g_{a_1}^{(2)}(0)$ and $g_{b_1}^{(2)}(0)$ are nearly zero over the entire range of g/κ. When Ω_p is absent, $g_{a_1}^{(2)}(0)$ and $g_{b_1}^{(2)}(0)$ remain one across the whole range of g/κ. This shows that the NPB in two optical modes emerges for a wide range of g/κ.

In Fig. 8(b), it can be found that the optimal nonreciprocity $I_{o,\mathrm{opt}}$ is linearly dependent on the logarithm of the signal-field amplitude E. Smaller signal-field amplitude generates a better nonreciprocity for photon blockade in two modes. The reason is that a large driving strength notably increases the probability occupation of the two-photon states $|20\rangle$ and $|02\rangle$, which weakens the photon antibunching. Under the parameters we propose, the nonreciprocal ratio of the two resonators achieves approximately 40 dB, indicating a good nonreciprocal blockade effect.

V. CONCLUSION

In conclusion, we investigated the simultaneously strong NPB in two microring resonators in an all-optical system, without the need for any rotating components. This is accomplished by unidirectionally parametrically pumping a $\chi^{(2)}$-nonlinear resonator using a classical coherent field. The counterclockwise mode in the resonator undergoes parametric amplification when a forward signal field is introduced into another resonator, while the amplification process does not occur for a backward signal field. As a result, distinct quantum interference effects emerge among different excitation paths for the two optical modes, which serves as the fundamental reason behind the simultaneous NPB. With the parametric amplification, we provide the optimal parameter conditions for simultaneously achieving strong PB of the two modes, which exhibits a good agreement with numerical results. Based on the analytical solutions, we find that the simultaneous NPB is controllable and enhanced by adjusting the driving field amplitude. Our work presents a promising approach to develop simultaneous nonreciprocal single-photon devices in multiple modes without any moving parts, making it easily implementable in experimental platforms, which holds potential applications in many-body quantum information processing.

ACKNOWLEDGMENTS

This work was supported by the Natural Science Foundation of Jilin Province under Grant No. 20240101013JC, and the National Natural Science Foundation of China under Grants No. 12375020, No. 12074330, No. 62071412, and No. 12074094.

[1] K. M. Birnbaum, A. Boca, R. Miller, A. D. Boozer, T. E. Northup, and H. J. Kimble, Photon blockade in an optical cavity with one trapped atom, Nature (London) **436**, 87 (2005).
[2] A. J. Shields, Semiconductor quantum light sources, Nat. Photon. **1**, 215 (2007).
[3] S. Ghosh and T. C. H. Liew, Dynamical blockade in a single-mode bosonic system, Phys. Rev. Lett. **123**, 013602 (2019).
[4] A. Imamoğlu, H. Schmidt, G. Woods, and M. Deutsch, Strongly interacting photons in a nonlinear cavity, Phys. Rev. Lett. **79**, 1467 (1997).
[5] D. Gerace, H. E. Türeci, A. Imamoglu, V. Giovannetti, and R. Fazio, The quantum-optical Josephson interferometer, Nat. Phys. **5**, 281 (2009).
[6] D. E. Chang, A. S. Sørensen, E. A. Demler, and M. D. Lukin, A single-photon transistor using nanoscale surface plasmons, Nat. Phys. **3**, 807 (2007).
[7] C. Sayrin, C. Junge, R. Mitsch, B. Albrecht, D. O'Shea, P. Schneeweiss, J. Volz, and A. Rauschenbeutel, Nanophotonic optical isolator controlled by the internal state of cold atoms, Phys. Rev. X **5**, 041036 (2015).
[8] L. Tang, J. Tang, W. Zhang, G. Lu, H. Zhang, Y. Zhang, K. Xia, and M. Xiao, On-chip chiral single-photon interface: Isolation and unidirectional emission, Phys. Rev. A **99**, 043833 (2019).
[9] C. Zhao, X. Li, S. Chao, R. Peng, C. Li, and L. Zhou, Simultaneous blockade of a photon, phonon, and magnon induced by a two-level atom, Phys. Rev. A **101**, 063838 (2020).
[10] C. J. Zhu, Y. P. Yang, and G. S. Agarwal, Collective multiphoton blockade in cavity quantum electrodynamics, Phys. Rev. A **95**, 063842 (2017).
[11] D. Y. Wang, C. H. Bai, X. Han, S. Liu, S. Zhang, and H. F. Wang, Enhanced photon blockade in an optomechanical system with parametric amplification, Opt. Lett. **45**, 2604 (2020).
[12] W. Zhang, S. Liu, S. Zhang, and H. F. Wang, Kerr-nonlinearity enhanced photon blockades via driving a Δ-type atom, Adv. Quantum Technol. **6**, 2300187 (2023).
[13] L. J. Feng, L. Yan, and S. Q. Gong, Unconventional photon blockade induced by the self-Kerr and cross-Kerr nonlinearities, Front. Phys. **18**, 12304 (2023).
[14] M. Bamba, A. Imamoğlu, I. Carusotto, and C. Ciuti, Origin of strong photon antibunching in weakly nonlinear photonic molecules, Phys. Rev. A **83**, 021802(R) (2011).
[15] X. W. Xu and Y. Li, Tunable photon statistics in weakly nonlinear photonic molecules, Phys. Rev. A **90**, 043822 (2014).
[16] D. Gerace and V. Savona, Unconventional photon blockade in doubly resonant microcavities with second-order nonlinearity, Phys. Rev. A **89**, 031803(R) (2014).

[17] J. Tang, W. Geng, and X. Xu, Quantum interference induced photon blockade in a coupled single quantum dot-cavity system, Sci. Rep. **5**, 9252 (2015).
[18] H. Flayac and V. Savona, Unconventional photon blockade, Phys. Rev. A **96**, 053810 (2017).
[19] T. C. H. Liew and V. Savona, Single photons from coupled quantum modes, Phys. Rev. Lett. **104**, 183601 (2010).
[20] W. Zhang, Z. Yu, Y. Liu, and Y. Peng, Optimal photon antibunching in a quantum-dot–bimodal-cavity system, Phys. Rev. A **89**, 043832 (2014).
[21] H. J. Snijders, J. A. Frey, J. Norman, H. Flayac, V. Savona, A. C. Gossard, J. E. Bowers, M. P. van Exter, D. Bouwmeester, and W. Löffler, Observation of the unconventional photon blockade, Phys. Rev. Lett. **121**, 043601 (2018).
[22] C. Vaneph, A. Morvan, G. Aiello, M. Féchant, M. Aprili, J. Gabelli, and J. Estève, Observation of the unconventional photon blockade in the microwave domain, Phys. Rev. Lett. **121**, 043602 (2018).
[23] H. Paul, Photon antibunching, Rev. Mod. Phys. **54**, 1061 (1982).
[24] C. Hamsen, K. N. Tolazzi, T. Wilk, and G. Rempe, Two-photon blockade in an atom-driven cavity QED system, Phys. Rev. Lett. **118**, 133604 (2017).
[25] T. Peyronel, O. Firstenberg, Q. Y. Liang, S. Hofferberth, A. V. Gorshkov, T. Pohl, M. D. Lukin, and V. Vuletić, Quantum nonlinear optics with single photons enabled by strongly interacting atoms, Nature (London) **488**, 57 (2012).
[26] Y.-x. Liu, X.-W. Xu, A. Miranowicz, and F. Nori, From blockade to transparency: Controllable photon transmission through a circuit-QED system, Phys. Rev. A **89**, 043818 (2014).
[27] D. Y. Wang, C. H. Bai, S. Liu, S. Zhang, and H. F. Wang, Distinguishing photon blockade in a $\mathcal{PT}$-symmetric optomechanical system, Phys. Rev. A **99**, 043818 (2019).
[28] D. Y. Wang, C. H. Bai, Y. Xing, S. Liu, S. Zhang, and H. F. Wang, Enhanced photon blockade via driving a trapped Λ-type atom in a hybrid optomechanical system, Phys. Rev. A **102**, 043705 (2020).
[29] C. H. Bai, D. Y. Wang, S. Zhang, and H. F. Wang, Qubit-assisted squeezing of mirror motion in a dissipative cavity optomechanical system, Sci. China Phys. Mech. Astron. **62**, 970311 (2019).
[30] W. Zhang, D. Y. Wang, C. H. Bai, T. Wang, S. Zhang, and H. F. Wang, Generation and transfer of squeezed states in a cavity magnomechanical system by two-tone microwave fields, Opt. Express **29**, 11773 (2021).
[31] M. Asjad, J. Li, S. Y. Zhu, and J. You, Magnon squeezing enhanced ground-state cooling in cavity magnomechanics, Fundamental Research **3**, 3 (2023).
[32] L. Wang, Z. X. Yang, Y. M. Liu, C. H. Bai, D. Y. Wang, S. Zhang, and H. F. Wang, Magnon blockade in a PT-symmetric-like cavity magnomechanical system, Ann. Phys. (Leipzig) **532**, 2000028 (2020).
[33] R. Huang, A. Miranowicz, J.-Q. Liao, F. Nori, and H. Jing, Nonreciprocal photon blockade, Phys. Rev. Lett. **121**, 153601 (2018).
[34] B. Li, R. Huang, X. Xu, A. Miranowicz, and H. Jing, Nonreciprocal unconventional photon blockade in a spinning optomechanical system, Photon. Res. **7**, 630 (2019).
[35] W. Zhang, T. Wang, S. Liu, S. Zhang, and H. F. Wang, Nonreciprocal photon blockade in a spinning resonator coupled to two two-level atoms, Sci. China Phys. Mech. Astron. **66**, 240313 (2023).
[36] Y. H. Zhou, H. Z. Shen, and X. X. Yi, Unconventional photon blockade with second-order nonlinearity, Phys. Rev. A **92**, 023838 (2015).
[37] H. Z. Shen, Y. H. Zhou, and X. X. Yi, Tunable photon blockade in coupled semiconductor cavities, Phys. Rev. A **91**, 063808 (2015).
[38] S. Ferretti, V. Savona, and D. Gerace, Optimal antibunching in passive photonic devices based on coupled nonlinear resonators, New J. Phys. **15**, 025012 (2013).
[39] H. Flayac and V. Savona, Input-output theory of the unconventional photon blockade, Phys. Rev. A **88**, 033836 (2013).
[40] O. Kyriienko and T. C. H. Liew, Triggered single-photon emitters based on stimulated parametric scattering in weakly nonlinear systems, Phys. Rev. A **90**, 063805 (2014).
[41] Y. H. Zhou, H. Z. Shen, X. Y. Zhang, and X. X. Yi, Zero eigenvalues of a photon blockade induced by a non-Hermitian hamiltonian with a gain cavity, Phys. Rev. A **97**, 043819 (2018).
[42] G. A. Peterson, F. Lecocq, K. Cicak, R. W. Simmonds, J. Aumentado, and J. D. Teufel, Demonstration of efficient nonreciprocity in a microwave optomechanical circuit, Phys. Rev. X **7**, 031001 (2017).
[43] L. Mercier de Lépinay, C. F. Ockeloen-Korppi, D. Malz, and M. A. Sillanpää, Nonreciprocal transport based on cavity floquet modes in optomechanics, Phys. Rev. Lett. **125**, 023603 (2020).
[44] M. Scheucher, A. Hilico, E. Will, J. Volz, and A. Rauschenbeutel, Quantum optical circulator controlled by a single chirally coupled atom, Science **354**, 1577 (2016).
[45] D. L. Sounas and A. Alù, Non-reciprocal photonics based on time modulation, Nat. Photon. **11**, 774 (2017).
[46] D. W. Zhang, L. L. Zheng, C. You, C. S. Hu, Y. Wu, and X. Y. Lü, Nonreciprocal chaos in a spinning optomechanical resonator, Phys. Rev. A **104**, 033522 (2021).
[47] H. Ramezani, P. K. Jha, Y. Wang, and X. Zhang, Nonreciprocal localization of photons, Phys. Rev. Lett. **120**, 043901 (2018).
[48] Q. T. Cao, H. Wang, C. H. Dong, H. Jing, R. S. Liu, X. Chen, L. Ge, Q. Gong, and Y. F. Xiao, Experimental demonstration of spontaneous chirality in a nonlinear microresonator, Phys. Rev. Lett. **118**, 033901 (2017).
[49] S. Manipatruni, J. T. Robinson, and M. Lipson, Optical nonreciprocity in optomechanical structures, Phys. Rev. Lett. **102**, 213903 (2009).
[50] Z. Shen, Y. L. Zhang, Y. Chen, C. L. Zou, Y. F. Xiao, X. B. Zou, F. W. Sun, G. C. Guo, and C. H. Dong, Experimental realization of optomechanically induced non-reciprocity, Nat. Photon. **10**, 657 (2016).
[51] Y. Xu, J. Y. Liu, W. Liu, and Y. F. Xiao, Nonreciprocal phonon laser in a spinning microwave magnomechanical system, Phys. Rev. A **103**, 053501 (2021).
[52] N. Bender, S. Factor, J. D. Bodyfelt, H. Ramezani, D. N. Christodoulides, F. M. Ellis, and T. Kottos, Observation of asymmetric transport in structures with active nonlinearities, Phys. Rev. Lett. **110**, 234101 (2013).
[53] L. Chang, X. Jiang, S. Hua, C. Yang, J. Wen, L. Jiang, G. Li, G. Wang, and M. Xiao, Parity-time symmetry and variable optical isolation in active-passive-coupled microresonators, Nat. Photon. **8**, 524 (2014).

[54] Y. L. Ren, Nonreciprocal optical–microwave entanglement in a spinning magnetic resonator, Opt. Lett. **47**, 1125 (2022).

[55] Q. Zheng, W. Zhong, G. Cheng, and A. Chen, Nonreciprocal tripartite entanglement based on magnon Kerr effect in a spinning microwave resonator, Opt. Commun. **546**, 129796 (2023).

[56] S. S. Chen, S. S. Meng, H. Deng, and G. J. Yang, Nonreciprocal mechanical squeezing in a spinning optomechanical system, Ann. Phys. (Leipzig) **533**, 2000343 (2021).

[57] K. W. Huang, Y. Wu, and L. G. Si, Parametric-amplification-induced nonreciprocal magnon laser, Opt. Lett. **47**, 3311 (2022).

[58] K. W. Huang, X. Wang, Q. Y. Qiu, L. Wu, and H. Xiong, Nonreciprocal phonon laser in an asymmetric cavity with an atomic ensemble, Chin. Phys. Lett. **40**, 104201 (2023).

[59] Y. J. Xu and J. Song, Nonreciprocal magnon laser, Opt. Lett. **46**, 5276 (2021).

[60] X. W. He, Z. Y. Wang, X. Han, S. Zhang, and H. F. Wang, Parametrically amplified nonreciprocal magnon laser in a hybrid cavity optomagnonical system, Opt. Express **31**, 43506 (2023).

[61] Z. Y. Wang, X. W. He, X. Han, H. F. Wang, and S. Zhang, Nonreciprocal PT-symmetric magnon laser in spinning cavity optomagnonics, Opt. Express **32**, 4987 (2024).

[62] W. S. Xue, H. Z. Shen, and X. X. Yi, Nonreciprocal conventional photon blockade in driven dissipative atom-cavity, Opt. Lett. **45**, 4424 (2020).

[63] Y.-W. Jing, H.-Q. Shi, and X.-W. Xu, Nonreciprocal photon blockade and directional amplification in a spinning resonator coupled to a two-level atom, Phys. Rev. A **104**, 033707 (2021).

[64] J. Wang, Q. Wang, and H. Z. Shen, Nonreciprocal unconventional photon blockade with spinning atom-cavity, Europhys. Lett. **134**, 64003 (2021).

[65] K. Wang, Q. Wu, Y. F. Yu, and Z. M. Zhang, Nonreciprocal photon blockade in a two-mode cavity with a second-order nonlinearity, Phys. Rev. A **100**, 053832 (2019).

[66] X. Shang, H. Xie, and X. M. Lin, Nonreciprocal photon blockade in a spinning optomechanical resonator, Laser Phys. Lett. **18**, 115202 (2021).

[67] H. Z. Shen, Q. Wang, J. Wang, and X. X. Yi, Nonreciprocal unconventional photon blockade in a driven dissipative cavity with parametric amplification, Phys. Rev. A **101**, 013826 (2020).

[68] Y. M. Liu, J. Cheng, H. F. Wang, and X. Yi, Simultaneous nonreciprocal conventional photon blockades of two independent optical modes by a two-level system, Phys. Rev. A **107**, 063701 (2023).

[69] C. Gou and X. Hu, Simultaneous nonreciprocal photon blockade in two coupled spinning resonators via Sagnac-Fizeau shift and parametric amplification, Phys. Rev. A **108**, 043723 (2023).

[70] J. R. Johansson, P. D. Nation, and F. Nori, QuTiP: An open-source Python framework for the dynamics of open quantum systems, Comput. Phys. Commun. **183**, 1760 (2012).